

Pervaporation Separation of Sodium Alginate/Chitosan Polyelectrolyte Complex Composite Membranes for the Separation of Water/Alcohol Mixtures: Characterization of the Permeation Behavior with Molecular Modeling Techniques

Sang-Gyun Kim, Ki-Sub Lee, Kew-Ho Lee

Membrane and Separation Research Center, Korea Research Institute of Chemical Technology, P.O. Box 107, Yuseong-Gu, Daejeon 305-606, South Korea

Received 17 March 2006; accepted 1 September 2006

DOI 10.1002/app.25386

Published online in Wiley InterScience (www.interscience.wiley.com).

ABSTRACT: Polyelectrolyte complex (PEC) membranes were prepared by the complexation of protonated chitosan with sodium alginate doped on a porous, polysulfone-supporting membrane. The pervaporation characteristics of the membranes were investigated with various alcohol/water mixtures. The physicochemical properties of the permeant molecules and polyion complex membranes were determined with molecular modeling methods, and the data from these methods were used to explain the permeation of water and alcohol molecules through the PEC membranes. The experimental results showed that the prepared PEC membranes had an excellent pervaporation performance in most aqueous alcohol solutions and that the selectivity and permeability of the membranes depended

on the molecular size, polarity, and hydrophilicity of the permeant alcohols. However, the aqueous methanol solutions showed a permeation behavior different from that of the other alcohol solutions. Methanol permeated the prepared PEC membranes more easily than water even though water molecules have stronger polarity and are smaller than methanol molecules. The experimental results are discussed from the point of view of the physical properties of the permeant molecules and the membranes in the permeation state. © 2006 Wiley Periodicals, Inc. *J Appl Polym Sci* 103: 2634–2641, 2007

Key words: metal-polymer complexes; polyelectrolytes; polysaccharides; self-assembly; separation techniques

INTRODUCTION

In recent years, polyelectrolyte complexes (PECs) have attracted special interest as membranes that can facilitate the separation of organic mixtures because of their high flux and selectivity for pervaporation dehydration.^{1,2} In general, PECs or polysalt complexes form when macromolecules of an opposite charge are allowed to interact. The interaction usually involves a polymeric acid or its salt with a polymeric base. Electrostatic interactions constitute the main attractive force, but hydrogen bonding, ion-dipole forces, and hydrophobic interactions frequently play significant roles in determining the ultimate structures. Accordingly, the permeability and permselectivity of permeants through membranes made from these complexes strongly depend on the chemical structures of the polymer components, the charge density, the ratio of the cationic charge to the anionic charge, the pH, the

presence of microions, and the procedures used in the complex preparation.

We have previously discussed how PEC-composite membranes composed of chitosan and sodium alginate (SA) can separate polar and nonpolar systems such as *tert*-methyl butyl ether/methanol mixtures. In addition, we have reported that to prepare a more stable complex membrane, the formation of PECs between these needs an interactive condition below a pK value of 2.0. Because of the physicochemical and structural properties, the membranes show better permselectivity for a polar constituent than for a nonpolar component.^{3–5}

Using PEC-composite membranes made of SA poly-anions and chitosan polycations, we studied the permeation behavior for the separation of polar-polar component mixtures, such as water and methanol, water and ethanol, and water and 2-propanol. We also used molecular modeling methods to investigate the morphologies of the resulting membranes at a molecular level and the physicochemical properties of the permeant molecules. Molecular dynamics simulation methods were used to study the microscopic characteristics of the membranes and the mechanisms of permeation.^{6,7}

Correspondence to: K.-H. Lee (khlee@kriect.re.kr).

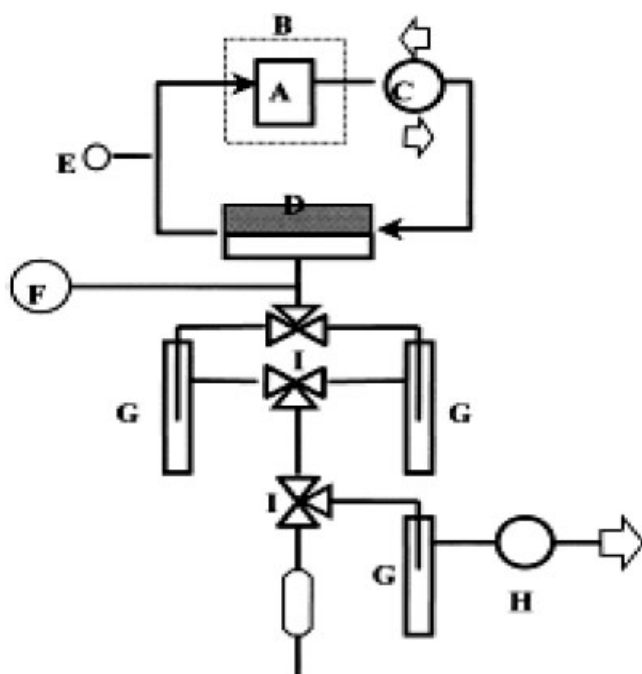


Figure 1 Schematic representation of the pervaporation device: (A) the feed tank, (B) the heating controller, (C) the pump, (D) the pervaporation cell, (E) the temperature indicator, (F) the pressure indicator, (G) the cold trap, (H) the vacuum pump, and (I) the three-way vacuum valve.

EXPERIMENTAL

Materials

SA and chitosan were purchased from Aldrich, Inc. (Milwaukee, WI), and the polysulfone membrane, with a molecular weight cutoff of 30,000, which supported the composite membranes, was purchased from UOP Corp. (San Diego, CA). The methanol (guaranteed reagent) was supplied by Merck (Darmstadt, Germany). From Junsei Chemical Co. (Tokyo, Japan), we purchased HCl (35%, extrapure grade), ethanol (guaranteed reagent), 2-propanol (IPA, guaranteed reagent), and *tert*-butyl alcohol (TBA, guaranteed reagent). Ultrapure, deionized water was used, and all chemicals were used without further purification.

Membrane preparation

SA was dissolved in deionized water to form a homogeneous solution of 2 wt % polymer. To prepare the composite-type PEC membranes, we first prepared homogeneous SA–composite membranes by dipping the skin layer of the polysulfone membranes into an SA solution and drying them at room temperature for 24 h in a dust-free, environmentally controlled chamber. A chitosan solution of 2.0 wt % was prepared by the dissolution of chitosan in water containing 5 wt % HCl. The overall prepared homogeneous SA–compos-

ite membranes were then immersed in a chitosan solution for 10 min. After the polyion complexation, the membranes were taken out of the chitosan solution, washed several times with pure water to eliminate any possible residual chitosan solution, and dried at room temperature.

Pervaporation measurements

Figure 1 shows our schematic permeation apparatus. The membrane cell was made of stainless steel. A feed mixture entered the cell through the center opening, flowed quickly through the thin channel, and exited the cell through the side opening, thereby allowing a relatively high fluid velocity parallel to the surface of the membrane. The effective membrane area was 19.6 cm². The feed mixture circulated from the feed tank, which had a capacity of 2.5 L, through the membrane cell. The feed tank was wrapped with heating tape to heat the feed mixture. The temperature of the feed mixture was controlled by a proportional-integral-derivative temperature controller with an accuracy of 0.5°C. A proportional-integral-derivative controller controlled the permeation pressure. The permeation vapor was collected in a cold trap by liquid nitrogen in a given time interval, heated to room temperature, and weighed to determine the flux. The separation analysis was conducted with a Shimadzu model GC 14B gas chromatograph (Tokyo, Japan) equipped with a thermal conductivity detector and a column packed

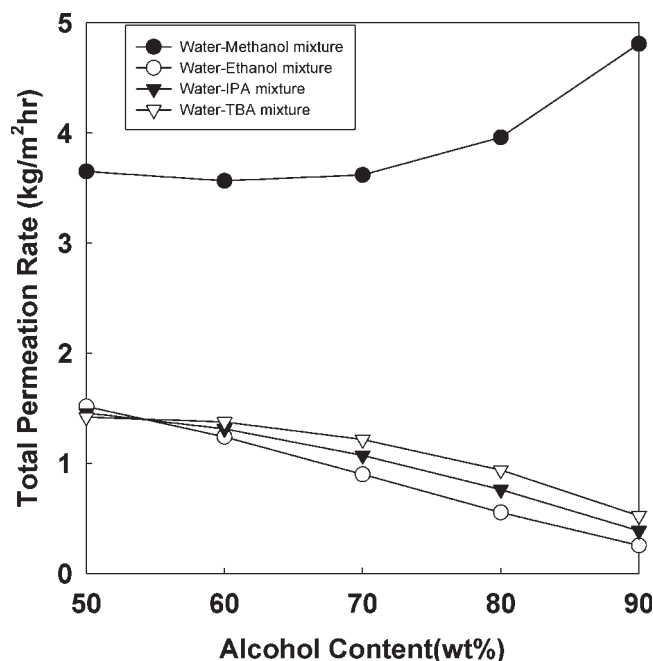


Figure 2 Total permeation rates of the prepared PEC composite membranes for the separation of water and alcohol mixtures as a function of the alcohol content in the feed at 40°C.

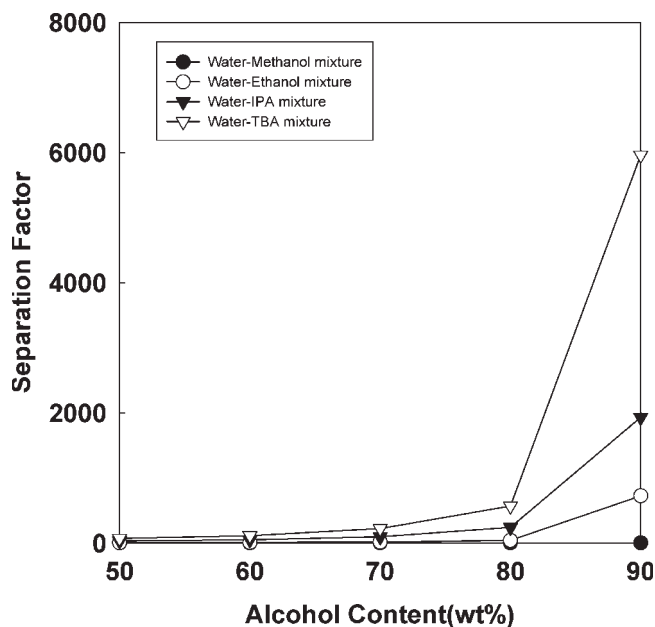


Figure 3 Separation factors of the prepared PEC composite membranes for the separation of water and alcohol mixtures as a function of the alcohol content in the feed at 40°C.

with Porapak-Q (Shimadzu, Kyoto, Japan). The separation factor ($\alpha_{\text{water/alcohol}}$) was calculated as follows:

$$\alpha_{\text{water/alcohol}} = (Y_{\text{water}}/Y_{\text{alcohol}})/(X_{\text{water}}/X_{\text{alcohol}})$$

where X and Y are the weight fractions of each component in the feed and permeate, respectively.

MOLECULAR MODELING

The molecular modeling of the bridging structure in the PEC membrane and in the permeant molecules was performed with the software packages Molecular Modeling (ChemSW, Inc., Fairfield, CA) and HyperChem (Hypercube, Inc., Gainesville, FL).

RESULTS AND DISCUSSION

For the separation of the various water/alcohol mixtures, Figures 2 and 3 show how the composition of the feed mixture affects the permeation rate and the separation factor of the PEC membranes composed of SA and chitosan. In the case of the water/methanol mixture, the permeation rate increases gradually as the alcohol concentration in the feed mixture increases, although the separation factor remains unchanged in a range of 0.77–0.46. For other water/alcohol mixtures, however, the permeation rate decreases and the separation factor increases with an increase in the alcohol content. At the same alcohol content, the total permeation rate almost increases

with an increase in the molecular weight of the alcohol component in the feed, except for methanol. The overall separation factors greatly increase with an increase in the molecular weight.

Generally, this result can be interpreted in terms of the plasticizing effect of water on the hydrophilic membrane and the coupling of fluxes by the interaction of the permeant molecules as the water concentration in the feed increases.^{8,9} The reason for this phenomenon is that the polymer chains become more flexible; consequently, the energy required for the diffusive transport through the membrane is reduced, and the diffusion is mainly through the

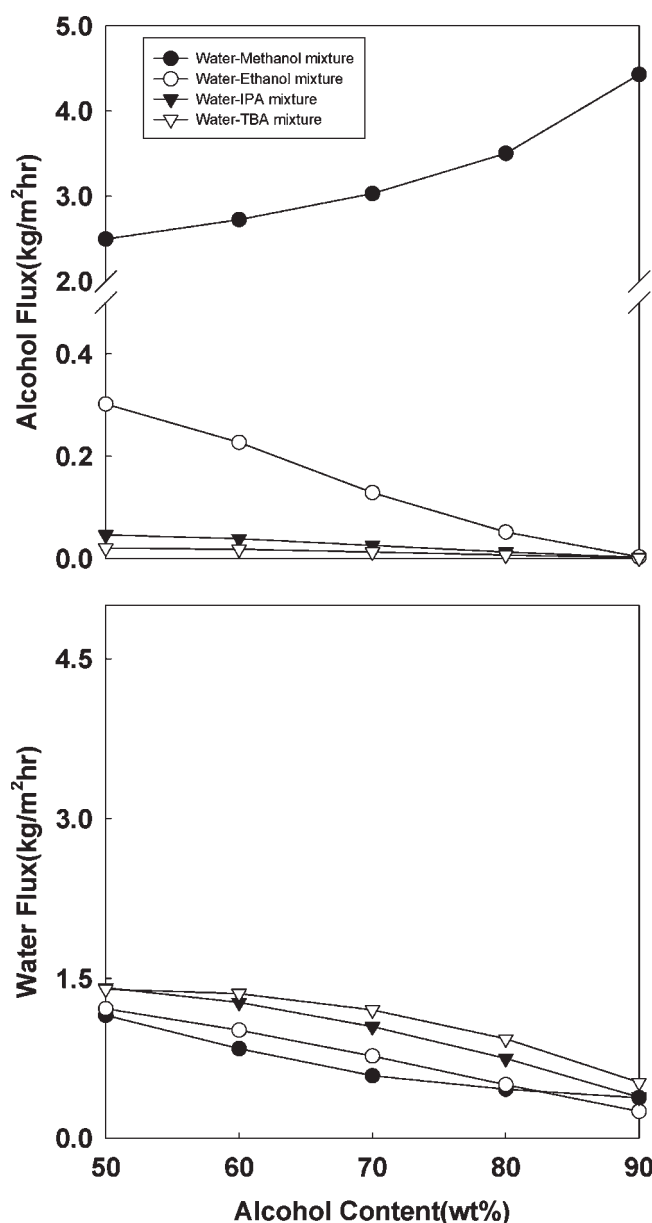


Figure 4 Individual component fluxes of the prepared PEC composite membranes for the separation of water and alcohol mixtures as a function of the alcohol content in the feed at 40°C.

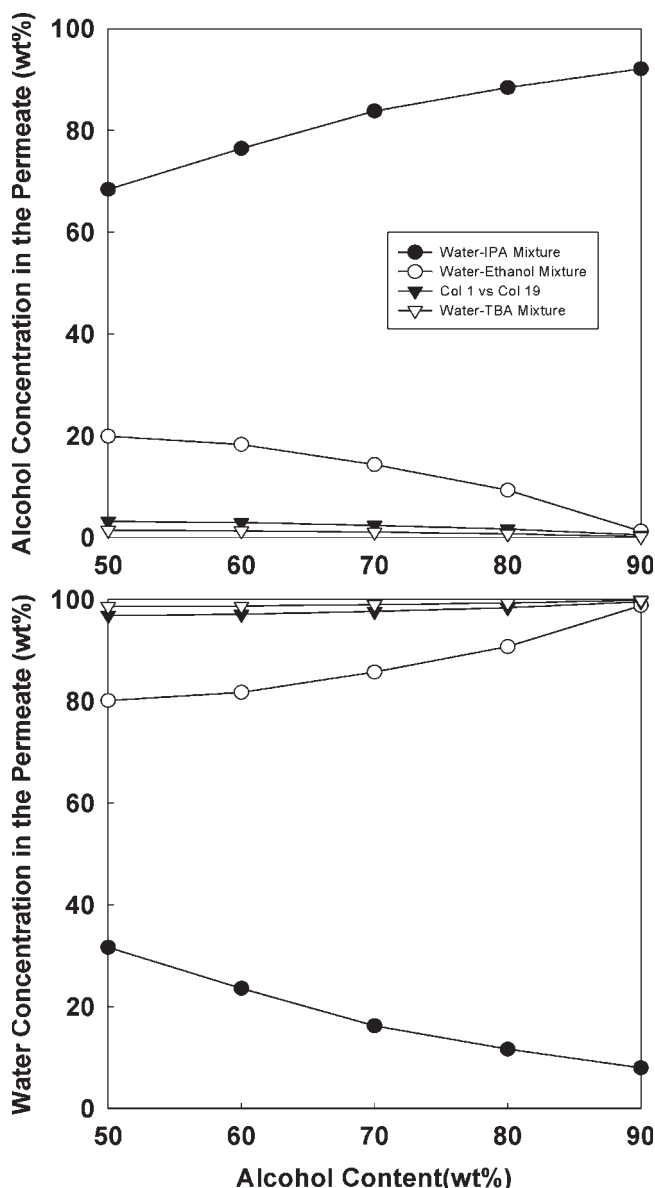


Figure 5 Individual permeation concentrations of the prepared PEC composite membranes for the separation of water and alcohol mixtures as a function of the alcohol content in the feed at 40°C.

swelling amorphous region in the membrane. In addition, the polar-polar constituent mixtures, such as methanol/water and ethanol/water, can also be subject to the interaction of polar groups. Finally, because the plasticizing effect of water increases the free volume of the membrane, the possibility of the interacted pairs and isolated molecules permeating through the membrane becomes greater, and the permeation rate of the alcohol component increases.

As shown in Figure 2, the permeation behavior suggests that the magnitude of the permeation rate in the low-alcohol region is influenced by the coupling fluxes between the polar groups and by the plasticization action of the water molecules. These results are sup-

ported by the permeation rate of each component and the concentration of the permeants in the permeate, as shown in Figures 4 and 5. That is, the alcohol concentration in the permeate increases gradually, whereas that of water decreases as the water content in the feed increases. As a result, the permeation rate of the alcohol component increases simultaneously with the increase in the water flux, but not for the methanol fluxes. Moreover, the increasing rate of the alcohol flux depends on the size of the molecules, and the plasticiz-

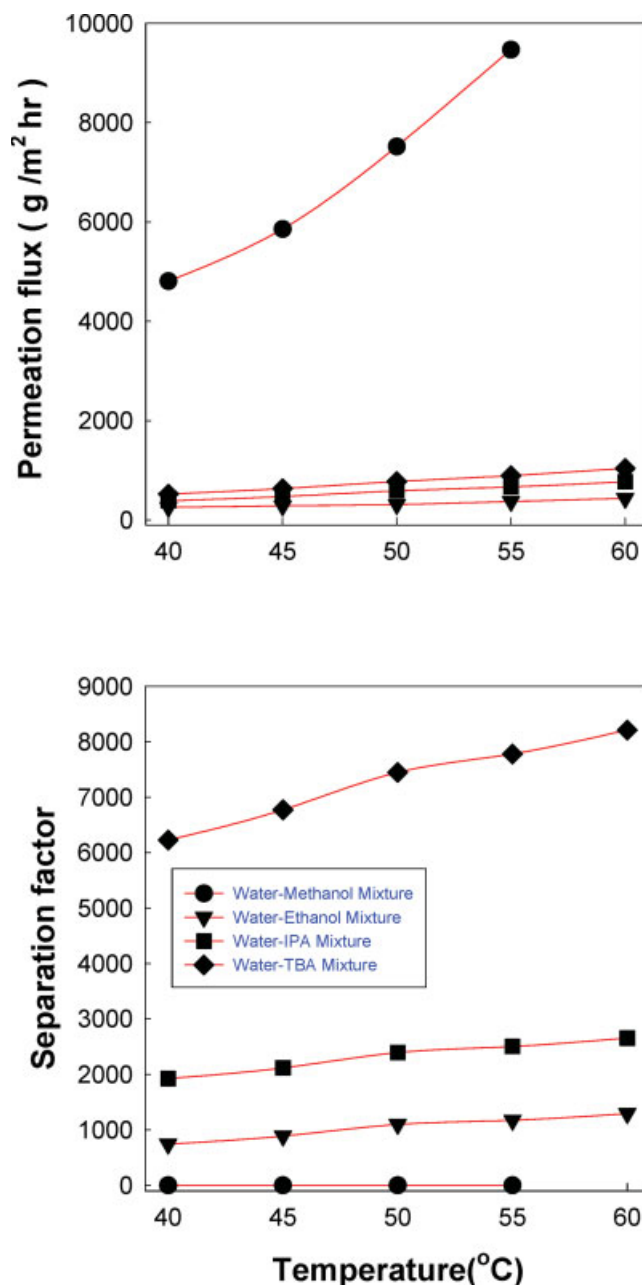


Figure 6 Permeation fluxes and separation factors of the prepared PEC composite membranes for the separation of water and alcohol mixtures as a function of the operating temperature. [Color figure can be viewed in the online issue, which is available at www.interscience.wiley.com.]

ing effect or coupling fluxes can therefore be attributed to the total permeation rate.

However, as shown in Figure 6, the effect of the operating temperature on the separation factor and on the permeation rate contradicts our remarks about the plasticizing action of water. Basically, the thermal motion of the polymer chains in the amorphous regions randomly produces a free volume, and the frequency and amplitude of the chain jumping increase as the temperature increases, thereby producing a larger free volume.¹⁰ Thus, when the operating temperature is high, the diffusion rates of the permeating molecules are high, and as a result,

the total permeation rate is high and the separation factor is low.

On the other hand, the interaction of permeants tends to weaken, and there is a greater possibility of reducing the associated unit size. This process forms more water molecules that are either isolated from or less associated with alcohol molecules. It also indicates that water molecules can permeate the membrane more extensively than alcohol, thereby increasing the separation factor. Consequently, the separation behavior can be affected by the segmental motion of the polymer chain and by the interaction between permeant molecules and the membrane.

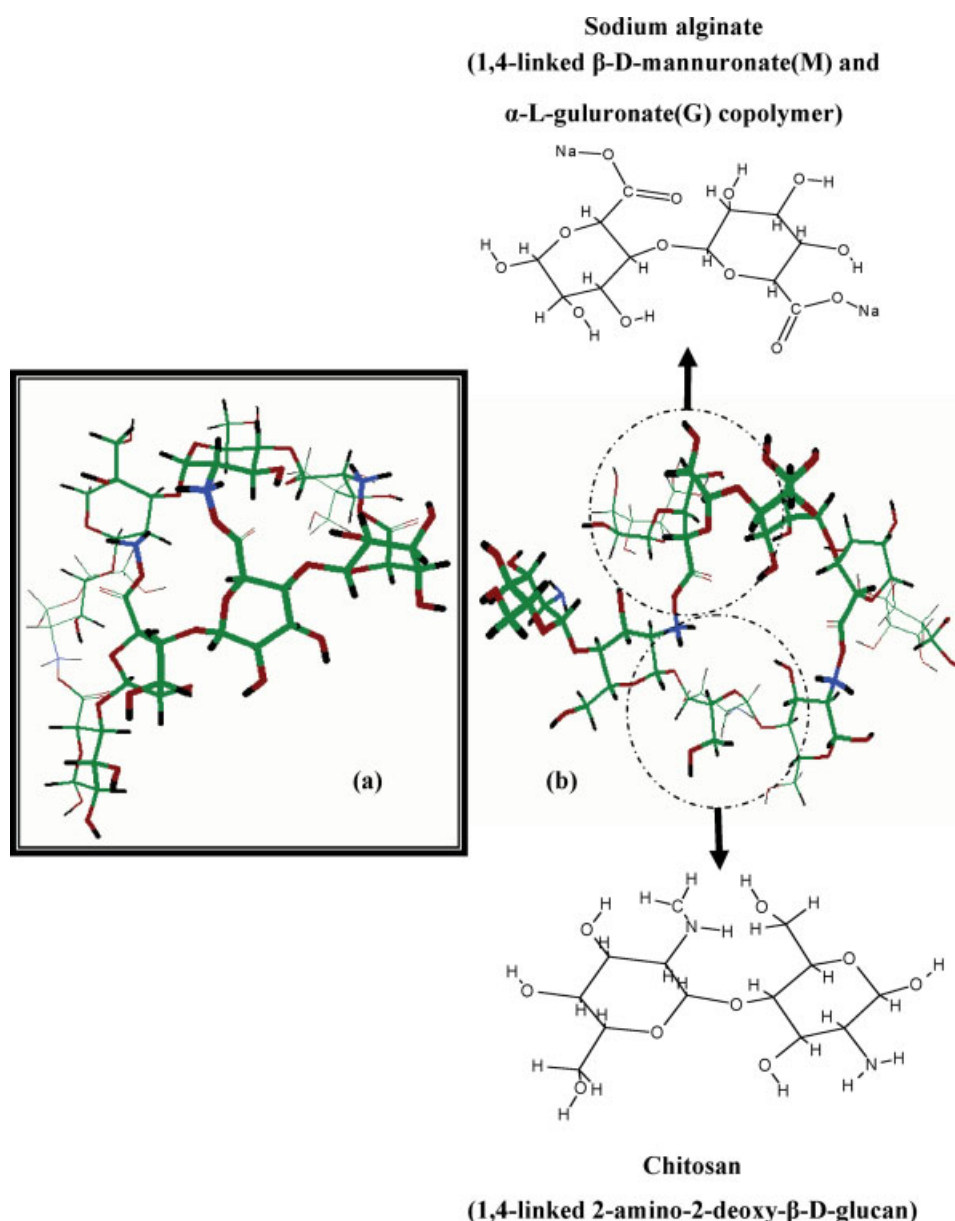


Figure 7 Molecular modeling results for the complex structure between SA and chitosan for (a) the simple ladder model and (b) the twofold-helix chain model (green = carbon, blue = nitrogen, red = oxygen, black = hydrogen). [Color figure can be viewed in the online issue, which is available at www.interscience.wiley.com.]

To consider these results more concretely, we used molecular modeling techniques, such as energy minimization and molecular dynamics, to examine the physicochemical relationship between the complex structure of the membrane and the permeants.

Chitosan is a polysaccharide polymer derived from α -chitin, and its repeating unit configuration is 1,4-linked 2-amino-2-deoxy- β -D-glucan.¹¹ Alginate is a copolymer that consists of linear chains of 1,4-linked β -D-mannuronate and α -L-guluronate residues

in various proportions.¹² The chain conformation of alginate manifests the following types: a twofold helix for polymannuronic acid, a threefold helix for sodium polymannuronate, and a twofold helix for polyguluronic acid.¹³

To construct these molecular structures, the Saccharide Builder of Hypercube was used. The conformation model is based on the molecular mechanics calculations for formable complex structures in relation to the cooperative ion-pair binding between the

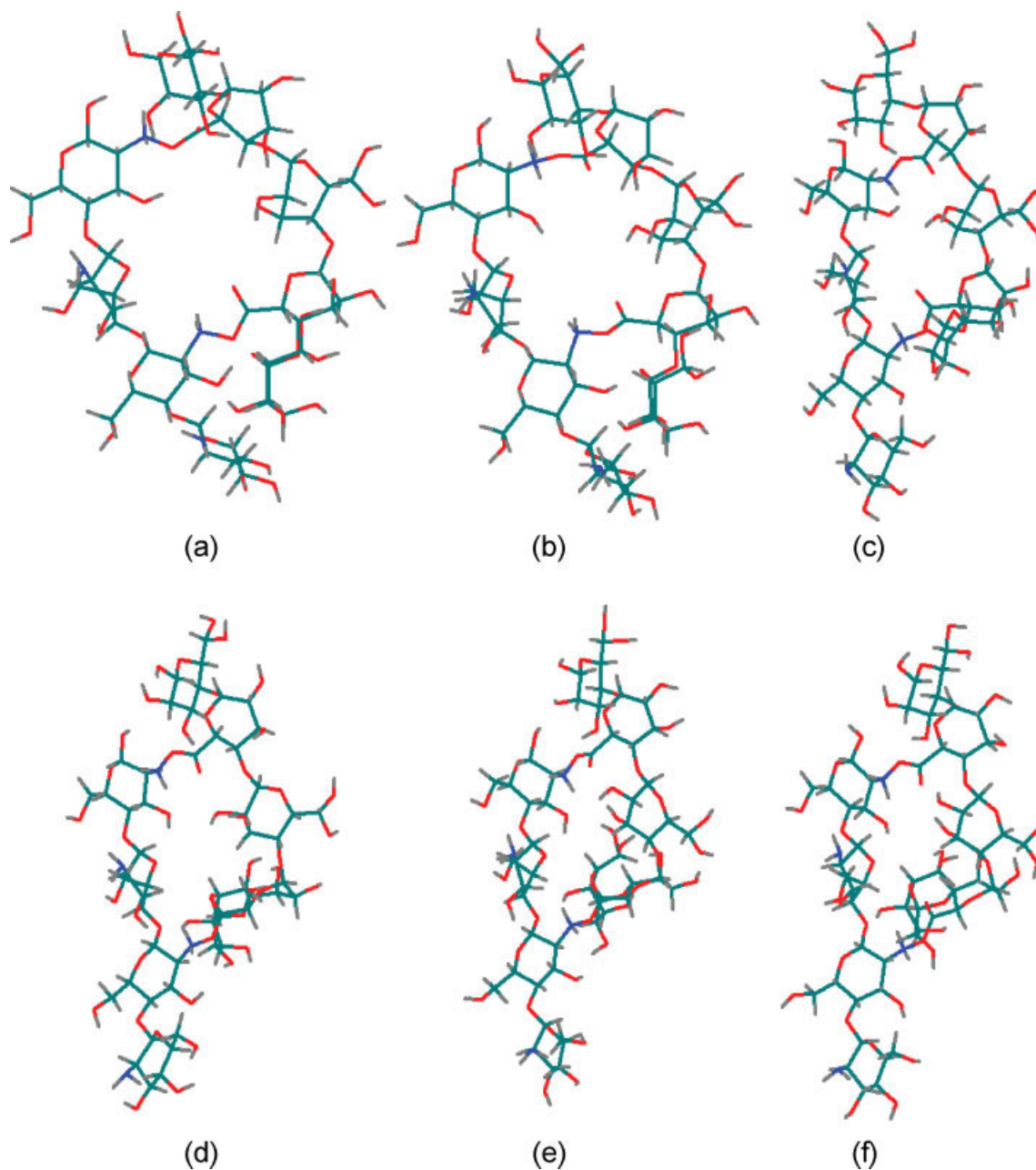
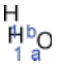
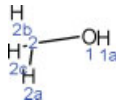
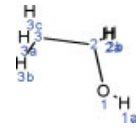
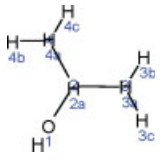
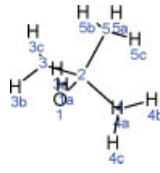


Figure 8 Molecular dynamics simulation results for the twofold-helix complex structure: (a) the complex model, (b) optimization results of the model at 298 K, (c) optimization results of the model at 300 K, (d) optimization results of the model at 308 K, (e) optimization results of the model at 318 K, and (f) optimization results of the model at 328 K (green = carbon, blue = nitrogen, red = oxygen, gray = hydrogen). [Color figure can be viewed in the online issue, which is available at www.interscience.wiley.com.]

TABLE I
Physicochemical Properties of Permeant Molecules Calculated with Molecular Modeling Methods

Property	H ₂ O	Methanol	Ethanol	Propan-2-ol	<i>t</i> -Butyl alcohol
Structure					
Interatomic distance (Å)	1a–1b: 1.5179 O1–1b: 0.9601	2a–1a: 2.8325 2b–2a: 1.7967	3c–1a: 4.0565 3b–2b: 3.0574	4b–3c: 4.2960 1a–3b: 3.8727	3c–4c: 4.2978 5a–1a: 3.4932
Molecular weight	18.0153	32.0422	46.0691	60.0959	74.1228
Molecular volume	11.2197	21.6731	31.612	41.5624	51.5311
Surface area	2.1758	3.61524	4.96094	6.30816	7.78356
Log P	–1.15	–0.768	–0.325	0.074	0.473
Solubility parameter	47.8	29.6107	26.4947	23.5076	21.6694
Dispersion	15.6	15.1106	15.7607	15.7552	15.3518
Hydrogen bonding	42.3	22.3057	19.3925	16.3379	14.2323
Polarity	16	12.285	8.80342	6.11979	5.59701
Hydrophilic surface (%)	100	60.8798	38.0249	22.0229	17.8596
Hydrogen-bond acceptor	0.573684	0.327753	0.332134	0.335396	0.33794
Hydrogen-bond donor	0.523684	0.227141	0.226308	0.225637	0.225148
Dipole moment	2.0032	1.65069	1.61491	1.66502	1.70173

carboxyl groups ($-\text{COO}^-$) of SA and the protonated amine groups ($-\text{NH}_3^+$) of chitosan.¹⁴ Thus, the designed molecules were optimized to a static structure via the steepest descent energy minimization until the maximum energy gradient of any atom was below 0.1 kcal/mol.

To confirm the structural characteristics for the operating temperature, a molecular dynamics simulation was conducted until we reached a range of 323–303 K. First, in the case of a complex conformer with a simple ladderlike structure, we observed a hole size in the 3.8–5.0-Å range in the ion-pair formation between SA and chitosan. When the conformer formed a twofold-helix alginate and chitosan with an α structure, the formation was in the magnitude of 4.5–5.5 Å, as shown in Figure 7. As shown in Figure 8, as the temperature of the molecular dynamics simulation increases, the size of the ion hole in these conformers gradually decreases because of the thermal motion of the polysaccharide chains and secondary interactions such as hydrogen bonding. This means that, because of the weakening interactions between the permeant molecules and the shrinking of the ion-pair volume between the polysaccharides, the separation factor increases as the operating temperature increases. As shown in Table I, when the alkyl chain of the alcohol molecule lengthens, its polarity and hydrogen-bonding ability dwindle.

The size of the alcohol molecules was generally greater than 3 Å, whereas the methanol was smaller than the complex structure's ion hole; in addition, the hydrogen-bonding ability was about half that of water. Accordingly, in the methanol/water system, the retention time of the methanol molecules at the

diffusion step was shorter than that of the water molecules because the physicochemical properties of the methanol molecules, such as the hydrophilic surface and the hydrogen-bonding ability, were lower than those of the water molecules, as can be seen in Table I.

Therefore, methanol molecules can permeate faster than water molecules. To confirm this result, individual permeation experiments for water and methanol were carried out, and we observed that methanol had a higher permeation rate than water (water, 4.118 kg/m² h; methanol, 9.490 kg/m² h). From these results, it was concluded that the desorption rate, which is related to the retention time of the permeants in the membrane, is a very important factor for the permeation of organic mixtures with similar physicochemical properties.

CONCLUSIONS

We used molecular modeling methods to elucidate the permeation characteristics of water/alcohol mixtures through SA–chitosan PEC membranes in a pervaporation process. The process was discussed in terms of the plasticizing effect and the interaction effect of the permeant molecules in the membrane. For the simple ladderlike structure in the ion-pair formation between SA and chitosan, the hole size ranged from 3.8 to 5.0 Å, and for the conformer, which was composed of twofold-helix alginate and chitosan with an α structure, the magnitude was in the range of 4.5–5.5 Å. When the temperature of the molecular dynamics simulation increased from 303 to 323 K, the hole size decreased gradually because of the thermal motion of the polysaccharide chains and secondary

interactions such as hydrogen bonding. In addition, through molecular modeling, we calculated the size of the alcohol molecules, and it was found that the size of methanol was smaller than that of the complex structure's ion hole. Accordingly, the selectivity and permeability of the membrane depended on the molecular size, polarity, and hydrophilic surface of the permeant organics. Therefore, for the aqueous methanol solution, the permeation behavior was different from that of the other alcohol solutions. This phenomenon was explained in terms of the chemical and physical properties of the permeant molecules and of the membrane in the diffusion state.

References

1. Peniche-Covas, C.; Argüelles-Monal, W.; Román, J. S. *Polym Int* 1995, 38, 45.
2. Ageev, E. P.; Kotova, S. L.; Skoikova, E. E.; Zezin, A. B. *Polym Sci Ser A* 1996, 38, 202.
3. Kim, S. G.; Lim, G. T.; Jegal, J.; Lee, K. H. *J Membr Sci* 2000, 174, 1.
4. Kim, S. G.; Kim, Y. I.; Jegal, J.; Lim, G. T.; Lee, K. H. *J Appl Polym Sci* 2002, 85, 1831.
5. Kim, S. G.; Kim, Y. I.; Lim, G. T.; Jegal, J.; Lee, K. H. *J Appl Polym Sci* 2002, 85, 714.
6. Allen, M. P.; Tildesley, D. J. *Computer Simulation of Liquids*; Oxford Science: Oxford, 1987.
7. Müller-Plate, F. *Acta Polym* 1994, 45, 259.
8. Huang, R. Y. M.; Lin, V. J. C. *J Appl Polym Sci* 1968, 12, 2615.
9. Brun, J. P.; Larchet, C.; Melet, M.; Bulvestre, G. *J Membr Sci* 1985, 23, 257.
10. Fujita, H. *Fortschr Hochpolym-Forsch* 1961, 3, 1.
11. *Applications of Chitin and Chitosan*; Goosen, M. F. A., Ed.; Technomic: Lancaster, PA, 1998.
12. Martinsen, A.; Skjåk-Braek, G.; Smidsrød, O. *Biotechnol Bioeng* 1989, 33, 79.
13. Atkins, E. D. T. In *Applied Fibre Science*; Harpey, F., Ed.; Academic: New York, 1983; Vol. 3, p 311.
14. Grant, G. T.; Morris, E. R.; Rees, D. A.; Smith, P. J. C.; Thom, D. *FEBS Lett* 1973, 32, 195.